

# Electrostatic Field Measurements and Band Flattening during Electron-Transfer Processes at Single-Crystal TiO<sub>2</sub> Electrodes by Electric Field-Induced Optical Second Harmonic Generation

Juliette M. Lantz and Robert M. Corn\*

Department of Chemistry, University of Wisconsin—Madison, 1101 University Ave., Madison, Wisconsin 53706

Received: January 21, 1994; In Final Form: March 4, 1994\*

Optical second harmonic generation (SHG) is employed as a local, time-resolved measurement of the electrostatic fields at the surface of single-crystal TiO<sub>2</sub> electrodes in contact with aqueous electrolyte solutions. The interfacial SHG at a fundamental wavelength of 584 nm is dominated by the electric field-induced second harmonic (EFISH) response from the first 20 nm of the space charge layer at the surface of the semiconductor. A substantial decrease in the amount of SHG from the electrode while under potentiostatic control is observed upon illumination of the surface with UV light (320 nm) whose energy is above the bandgap for TiO<sub>2</sub> (3.0 eV or 410 nm). Comparisons of the drop in SHG upon UV illumination with photovoltage measurements for TiO<sub>2</sub> electrodes at open circuit verify that this decrease is due to a reduction in the strength of the electrostatic fields ("band flattening") within the space charge region upon UV illumination. The EFISH response from the surface decreases with increasing power of the UV illumination, corresponding to a band flattening of up to 70% for the highest power densities. Upon termination of the UV illumination, a slow (10–12 s) rise time is observed for the return of the surface SHG to its normal levels. The unexpected length of this rise time is attributed to the chemical discharge of surface charge trap sites on the semiconductor electrode surface and can be shortened considerably by the addition of a hole scavenger such as sodium sulfite to the electrolyte solution.

## I. Introduction

The photoelectrochemical splitting of water on TiO<sub>2</sub> by Fujishima and Honda in 1972<sup>1</sup> initiated a flurry of experiments on this semiconductor electrode in the hope that it would become a viable material for use in solar energy conversion systems.<sup>2,3</sup> Over 20 years later, TiO<sub>2</sub> is still used extensively in a variety of photochemical applications including the storage and generation of energy.<sup>4–7</sup> Due to its large bandgap (3.0 eV), TiO<sub>2</sub> is capable of oxidizing a wide variety of organic and inorganic compounds.<sup>2</sup> The ability of the TiO<sub>2</sub> surface to resist photooxidation has made it an exceedingly useful photocatalyst;<sup>8,9</sup> however, the exact nature of the surface photocatalytic properties of TiO<sub>2</sub> electrodes still remains a subject of significant debate and controversy.<sup>2,10</sup>

Many experimental techniques have been applied to the study of the TiO<sub>2</sub>/electrolyte interface in an attempt to elucidate the various contributions of the bulk and surface properties to the electrode's reactivity. The earliest works were mainly electrochemical in nature<sup>2,11</sup> and were driven by the need to prepare TiO<sub>2</sub> electrodes with stable and reproducible photoelectrochemistry. These early studies demonstrated that the photoelectrochemical response of TiO<sub>2</sub> electrodes exhibited a complex dependence on surface polishing, crystal doping, and surface etching.<sup>2</sup> As a result of the electrochemical studies involving various redox species, it was postulated that the mechanism of charge transfer across the interface involved either surface states or adsorbed surface intermediates.<sup>12,13</sup> These issues prompted the need for *in situ* surface analysis, and various spectroscopic techniques were subsequently employed to provide information on surface structure and reaction kinetics at TiO<sub>2</sub> electrodes.<sup>11,14–17</sup> Most recently, scanning tunneling microscopy has been applied to the study of single-crystal TiO<sub>2</sub> surfaces.<sup>18,19</sup> In order to create more efficient photocatalysis systems, the various physical inhomogeneities of the TiO<sub>2</sub> electrode surface need to be assigned to various aspects of the surface reactivity. Furthermore, the detailed mechanisms of charge accumulation and charge transfer must be probed further to promote efficient use of this valuable photoelectrochemical interface. This work endeavors to provide

insight into these processes by using optical second harmonic generation to directly probe the electrostatic fields at the TiO<sub>2</sub> surface.

To correlate the measurements of the dc electric fields present at the semiconductor/electrolyte interface with the current understanding of photoelectrochemical processes, it is first necessary to consider the origins of this electric field and its influence on the various photoelectrochemical parameters. When a semiconductor electrode is immersed in a concentrated electrolyte solution, charge moves to the interface so as to equalize the two Fermi levels. This buildup of surface charge creates an interfacial double layer.<sup>20</sup> On the solution side, the excess interfacial charge is compensated over a short distance by the high number of mobile charge carriers present in a concentrated electrolytic solution. In contrast, the relatively low number of charge carriers on the semiconductor side of the interface means that full charge compensation must occur over a much longer distance (Figure 1a).<sup>2</sup> This region where the surface charge distribution differs from the bulk distribution is termed the space charge layer; for a TiO<sub>2</sub> electrode with a doping density of 10<sup>16</sup> dopants cm<sup>-3</sup> and a potential drop across the interface of 1.0 V, this space charge layer is on the order of 1 μm.<sup>2</sup> As depicted in Figure 1b, the charge distribution in the space charge layer generates a potential drop that is a function of distance,  $V(x)$ , at the semiconductor surface.<sup>21,22</sup> The total drop in potential across the space charge region from the surface to the bulk is termed band bending, which we will denote  $\Delta V_{sc}$ . When  $\Delta V_{sc} = 0$ , there is no band bending, and the electrode is at its characteristic flatband potential ( $V_{fb}$ ). The distribution of charge at the semiconductor surface also creates a dc electric field in the space charge layer. As the gradient of the potential, the electric field is at a maximum at the semiconductor surface and decreases further into the space charge layer in an approximately linear fashion, as shown in Figure 1c.<sup>22</sup> Once the electric fields have been established at the surface, they will dictate the movement of any mobile charge carriers either toward or away from the surface, depending upon the sign of the carrier charge. For an n-doped TiO<sub>2</sub> electrode, the electric fields are strongest at potentials positive of the flatband potential (the "depletion

\*Abstract published in *Advance ACS Abstracts*, April 1, 1994.

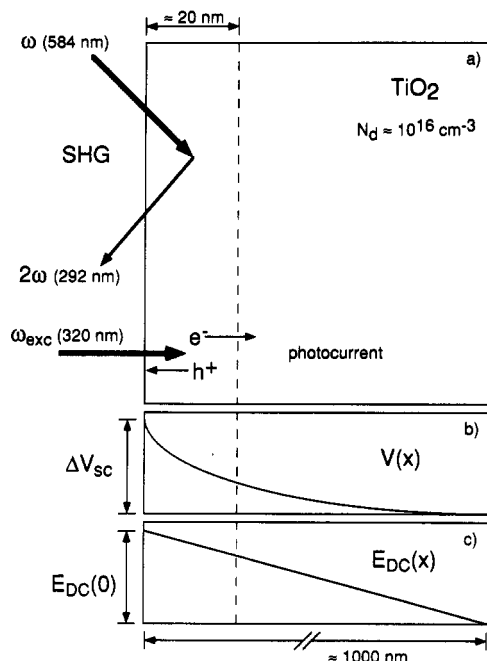


**Figure 1.** Schematic diagram of the n-doped TiO<sub>2</sub> semiconductor/electrolyte interface. (a) At potentials positive of the flatband potential, the space charge layer can extend on the order of 1  $\mu\text{m}$  into the semiconductor. UV light at  $\approx 300$  nm, however, is energetically above the bandgap for TiO<sub>2</sub> and as a result is strongly absorbed by the electrode. Thus, (i) the escape depth for the second harmonic signal at 292 nm is only  $\approx 20$  nm, and (ii) the excitation light at 320 nm is also strongly absorbed, so that the photogenerated  $e/h$  pairs are only found in this same 20-nm region. (b) Voltage profile *vs* distance in the depletion region.  $\Delta V_{\text{sc}}$  is the total potential drop or band bending across the space charge layer. (c) The corresponding dc electric field profile at the semiconductor surface. The electric fields at the surface cause photogenerated holes to be driven toward the interface and electrons to be driven through the circuit, resulting in a net photocurrent.

region”), while at the flatband potential the electric fields are essentially zero.

The electric fields at the surface of a semiconductor electrode govern its photoelectrochemical response.<sup>23</sup> When a semiconductor is illuminated with light whose energy is greater than the bandgap energy (suprabandgap light), mobile charge carriers in the form of electron/hole ( $e/h$ ) pairs are generated. These  $e/h$  pairs can either undergo immediate recombination or, in the presence of an electric field, move under the field’s influence and consequently be separated across the space charge layer. For TiO<sub>2</sub> electrodes illuminated with suprabandgap light at 320 nm, the  $e/h$  pairs are only created within the first 20 nm of the space charge layer, because the 320-nm light is strongly absorbed by the TiO<sub>2</sub> crystal (see Figure 1a). Using an absorption coefficient<sup>2</sup> of  $8 \times 10^5 \text{ cm}^{-1}$ , the penetration depth for this light is approximately 20 nm, and it is therefore expected that the majority of the  $e/h$  pairs are created within the first 20 nm of the electrode adjacent to the electrolyte interface. The electric field that is present in this spatial region when the electrode is biased positive of  $V_{\text{fb}}$  drives the photogenerated electrons into the bulk of the electrode, while the holes travel to the surface.

When charge separation does take place, the accumulation of holes at the electrode surface neutralizes a portion of the charge present in the space charge layer. This results in an effective decrease in the electric fields from their initial magnitude before suprabandgap illumination.<sup>2,21</sup> Concomitant with the decrease in the electric fields is a decrease in  $\Delta V_{\text{sc}}$ , the potential drop across the space charge layer; this decrease is referred to as band flattening. The generation and separation of charge at a semiconductor electrode also give rise to two distinct photoelectrochemical responses. In an open circuit configuration, the accumulation of holes at the electrode surface results in a decrease

in both the electric fields and the rest potential of the electrode. The change in the rest potential of the electrode that is caused by illumination with suprabandgap light is termed  $V_{\text{ocp}}$ , the open circuit photovoltage. Its value depends upon the solution potential that is set by the various redox species in the aqueous phase,<sup>2,23–25</sup> and in the case of intense illumination (when complete band flattening occurs),  $V_{\text{ocp}}$  can be used to approximate  $V_{\text{fb}}$ .<sup>2,3</sup> The second measurable photoelectrochemical parameter, the photocurrent, can only be monitored in a closed circuit configuration. In this case, the charge separation brought about by the dc electric fields present at the surface results in a steady-state concentration of holes at the electrode surface that oxidize solution species while the electrons are driven back through the circuit, resulting in a net photocurrent through an external circuit. For TiO<sub>2</sub> in the absence of any added redox solution species, water is the species that is oxidized into O<sub>2</sub> and other photoproducts, although the mechanisms for these reactions are not completely understood.<sup>2,16,26–30</sup> In the photocurrent measurements, the steady-state concentration of holes at the electrode surface still results in band flattening; however, due to the closed circuit configuration necessary for the measurement, the magnitude of the band flattening is unobtainable by electrochemical methods. Regardless of the measurable electrochemical parameter, photovoltage or photocurrent, the fundamental property determining the energetics of the charge generated by the suprabandgap light is the dc electric field in the semiconductor space charge layer. The electric field is indicative of the charge accumulation at the semiconductor surface, it controls charge separation, and any changes in the electric field at the surface can be directly related to charge-transfer events.

In our previous paper, we demonstrated that the nonlinear technique of optical second harmonic generation (SHG) can be used as a probe of the electric fields for TiO<sub>2</sub> electrodes *in situ*.<sup>31</sup> The SHG process involves the conversion of two photons at frequency  $\omega$  to one photon of frequency  $2\omega$ ; to a good approximation, this conversion can only take place in a region that is noncentrosymmetric such as the interface of a solution and a centrosymmetric crystal.<sup>32–38</sup> In the case of the TiO<sub>2</sub> semiconductor/electrolyte interface, the electric fields at the semiconductor surface break the symmetry of the crystal throughout the space charge region, which causes a large SHG response from the TiO<sub>2</sub> electrode. This mechanism is called electric field-induced SHG (EFISH).<sup>39</sup> At the wavelengths chosen for our experiments, the second harmonic light at  $2\omega$  (292 nm or 4.25 eV) falls above the bandgap of TiO<sub>2</sub> and as a result is strongly absorbed by the TiO<sub>2</sub> crystal. Once again, the extinction coefficient for this wavelength can be used to calculate an escape depth of approximately 20 nm as shown in Figure 1a.<sup>2</sup> Therefore, EFISH directly probes only the dc electric fields in the first 20 nm of the TiO<sub>2</sub> surface. In our previous work,<sup>31</sup> we established the relationship between the SHG signal and the dc surface electric fields and the relationships between the electric fields at the surface, the band bending  $\Delta V_{\text{sc}}$ , and the charge on the electrode. Through those experiments it was ascertained that the SHG response had a direct and linear relationship to the value of  $\Delta V_{\text{sc}}$  at the electrode surface.

This paper uses EFISH to study the dc electric fields and band bending of an n-TiO<sub>2</sub> semiconductor electrode under suprabandgap excitation. The experimental configuration is depicted schematically in Figure 2. When the SHG probe beam overlaps with the UV excitation source spatially, a sharp drop in SHG intensity is observed due to the reduction in electric fields at the TiO<sub>2</sub> surface. This measurement is made in two distinct modes. First, with an applied potential, the decreased EFISH response is related to the band flattening (i.e., the decrease in  $\Delta V_{\text{sc}}$ ) during the flow of current within the UV spot; thus, the magnitude of the band flattening can be compared to the concomitant photocurrent arising from the same region.<sup>31</sup> The values for the

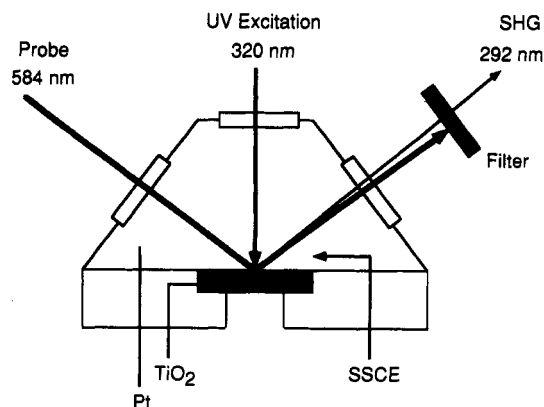


**Figure 2.** Experimental configuration for the *in situ* SHG measurements from a n-TiO<sub>2</sub> surface in an electrochemical cell under UV illumination. The p-polarized fundamental SHG beam (probe) is at 584 nm and is 60° from the surface normal. The normally incident pump beam has a wavelength of 320 nm. The two beams are overlapped spatially on the surface in a ≈200-μm spot.

optically determined band flattening are reported as a function of potential and UV power. Additionally, an unusually slow return time of the electric fields to their original value upon termination of the UV excitation indicates the presence of surface charge traps;<sup>40</sup> the effect of these traps is shown to be minimized by the addition of a hole scavenging species such as sulfite. In a second mode of experiments, the SHG response is measured concurrently with the photovoltage from an open circuit n-TiO<sub>2</sub> electrode interface. In this case, the optically determined band flattening is shown to be equivalent to the open circuit photovoltage measured electrochemically, both in the magnitude of the potential drop upon illumination and in the time required to return the electric fields to their equilibrium value. This open circuit measurement serves to verify that the EFISH response from the TiO<sub>2</sub> electrode with an applied potential is a direct measurement of the band flattening process.

## II. Experimental Considerations

The SHG experiments were performed *in situ* on n-doped single crystal TiO<sub>2</sub> (001) electrodes in the experimental arrangement depicted in Figure 2. The 584-nm output of a pulsed dye laser (4-MHz repetition rate, 3-ps pulse width, 25-nJ pulse energy) was focused to a 150-μm spot on the electrode surface with an incident angle of 60° from the surface normal. This probe beam was polarized parallel to the plane of incidence (p-polarization). Second harmonic light at 292 nm generated at the electrode surface from the 584-nm probe beam was separated from the reflected fundamental light and detected with a cooled photomultiplier tube and gated photon-counting electronics with a 1-s rise time. Both p-polarized and s-polarized (polarized perpendicular to the plane of incidence) SHG were detected. A more detailed description of the SHG experimental apparatus has been given elsewhere.<sup>41</sup>

The suprabandgap excitation beam that was used to produce changes in the surface SHG was focused onto the electrode at normal incidence (Figure 2). This UV beam was the doubled output at 320 nm from a 640-nm pulsed dye laser identical to that used for the SHG probe beam (0.4-nJ pulse energy, 400-μm spot size, power density 375 mW cm<sup>-2</sup>). Although the SHG probe beam and the excitation beam were overlapped spatially, they were not overlapped temporally. Arranging for the pair of picosecond pulses to arrive at the surface at exactly the same time leads to transient effects that will be a subject of a future paper.<sup>42</sup> In this paper, however, the delay between the two pulses was set to at least 26 ns to simulate a steady-state measurement. For confirmation of this steady-state system approximation, the CW output of a HeCd laser (Omnichrome, Series 56) at 325 nm

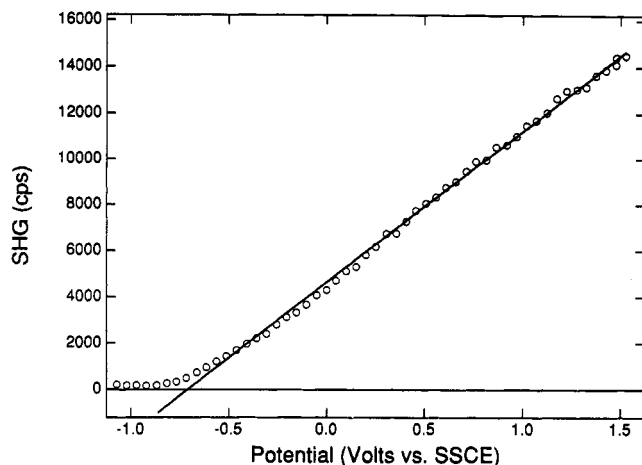


**Figure 3.** Potential dependence of the SHG signal at 292 nm from an n-TiO<sub>2</sub> electrode in the absence of illumination. The supporting electrolyte is 0.3 M NaClO<sub>4</sub> + 10 mM Na<sub>2</sub>HPO<sub>4</sub>, with the pH of the phosphate buffer set to 7. The large linear increase in SHG observed at potentials positive of the flatband potential is attributed to the EFISH response of the TiO<sub>2</sub> semiconductor in the space charge layer.

was also used in a set of SHG pump-probe experiments; in these comparison experiments, both the CW and the pulsed UV excitation sources yielded the same experimental results.

The n-TiO<sub>2</sub> electrodes were prepared by reduction in a heated H<sub>2</sub>/N<sub>2</sub> atmosphere as described previously and were determined to have donor densities of 10<sup>15</sup>–10<sup>16</sup> dopants cm<sup>-3</sup>.<sup>31</sup> The electrochemical measurements on the n-TiO<sub>2</sub> electrodes were obtained and controlled with a Princeton Applied Research 173/175 potentiostat in a three-electrode Teflon cell using a Pt counter electrode and a NaCl-saturated calomel reference electrode (SSCE); all potentials are reported versus SSCE. Solutions were prepared from Millipore-filtered water and contained 0.1–0.3 M NaClO<sub>4</sub> (Aldrich) as the supporting electrolyte along with either 10 mM Na<sub>2</sub>HPO<sub>4</sub> (Fluka) or 1 mM Na<sub>2</sub>SO<sub>3</sub> (Fisher Scientific). The pH of the electrolyte solutions was controlled by adjusting the buffers with either HClO<sub>4</sub> (GFS Chemicals) or NaOH (Fluka).

## III. Results and Discussion

**A. EFISH Response from Semiconductor Electrodes.** The surface SHG from an n-doped TiO<sub>2</sub> electrode at a fundamental wavelength of 584 nm is plotted as a function of applied potential in Figure 3 in the absence of UV illumination. As reported in our previous paper,<sup>31</sup> a very large second harmonic response is observed at potentials positive of the flatband potential due to the presence of a space charge layer at the semiconductor interface. This large second harmonic response varies linearly with applied potential and is attributed to an electric field-induced second harmonic (EFISH) response from the polarization of the TiO<sub>2</sub> crystal lattice by the electric fields in the space charge layer. Since the second harmonic wavelength (292 nm) is strongly absorbed by the sample, only the first ≈20 nm of the space charge layer contributes to the reflected surface SHG signal. The observed surface SHG intensity  $I(2\omega)$  is proportional to the square of the magnitude of the surface nonlinear polarization  $P^{(2)}(2\omega)$  induced within this layer<sup>39,40,43–45</sup>

$$P^{(2)}(2\omega) = (\chi^{(2)} + \chi^{(3)} \cdot E_{dc}) \cdot E(\omega) \cdot E(\omega) \quad (1)$$

where  $\chi^{(2)}$  is the second-order nonlinear susceptibility of the surface in the absence of electrostatic fields and  $\chi^{(3)}$  is the third-order nonlinear hyperpolarizability that relates the three input electric fields, two at frequency  $\omega$  and one at zero (dc) frequency, to the surface nonlinear polarization at frequency  $2\omega$ . Hyperpolarizability contributions to the SHG from semiconductor

surfaces have been observed previously.<sup>39,40,46</sup> For the n-TiO<sub>2</sub> electrodes, we have found that the hyperpolarizability contributions ( $\chi^{(3)}:E_{dc}$ ) dominate the surface contributions ( $\chi^{(2)}$ ) to the nonlinear polarization in the depletion region. At potentials negative of the flatband potential (the "accumulation region"), the EFISH response of the TiO<sub>2</sub> surface is greatly reduced since the depth of the space charge layer is minimized.<sup>2,21</sup>

The linear potential dependence of the EFISH response from TiO<sub>2</sub> electrodes in the depletion region observed in Figure 3 can be explained with a simple (Mott-Schottky) model of the interface.<sup>20,22,47</sup> Using this simple model, eq 2 relates the excess charge in the space charge layer,  $q_{sc}$ , to  $\Delta V_{sc}$ , the difference between the applied potential and the flatband potential (the band bending) at the interface<sup>47</sup>

$$q_{sc} = (2\epsilon\epsilon_0eN_d)^{1/2}\Delta V_{sc}^{1/2} \quad (2)$$

where  $N_d$  is the doping density,  $\epsilon$  is the dielectric constant of TiO<sub>2</sub> (perpendicular to the  $c$  axis), and all other symbols have their usual meaning. From Gauss' law, the magnitude of the electrostatic fields at the surface of the space charge layer ( $E_{dc}$ ) is directly proportional to the total charge  $q_{sc}$ .<sup>20,22</sup> Since the SHG intensity depends upon the square of the magnitude of the electrostatic fields (from eq 1), we find that the SHG from the electrode surface should vary linearly with applied potential.

$$I(2\omega) \propto |E_{dc}|_{x=0}^2 \propto q_{sc}^2 \propto \Delta V_{sc} \quad (3)$$

The potential at which the surface SHG reaches a minimum is that point at which  $q_{sc} = 0$ ; this potential is the optically measured flatband potential for the semiconductor/electrolyte interface<sup>31</sup> and is  $-0.73$  V for the n-TiO<sub>2</sub> electrode used for the experiments in Figure 3.

**B. Band Flattening and Photocurrent Measurements.** Illumination of the electrode surface with UV light at 320 nm results in the formation of electron/hole pairs in the first 20 nm of the semiconductor surface. If the electrode is held at a potential positive of the flatband potential, these electron/hole pairs are separated by the electric fields in the space charge region and give rise to a measurable photocurrent as the holes are consumed at the semiconductor/electrolyte interface. The steady-state concentration of photogenerated holes at the surface is expected to decrease both the interfacial electric fields and the concomitant band bending,  $\Delta V_{sc}$ , at the interface. This effect is termed band flattening; it can be monitored simultaneously with the photocurrent by measuring the changes in the SHG from the semiconductor electrode upon illumination.

The photocurrent and surface SHG from a n-TiO<sub>2</sub> electrode held at a potential of +0.5 V are plotted in Figure 4 as a function of time during three separate periods of UV (320 nm) illumination on the surface. During the third illumination period, the 584-nm SHG probe beam is blocked briefly in order to verify that no scattered 320-nm light is contributing to the SHG signal at 292 nm. In each of the three UV illumination periods, a large drop in the surface SHG is observed concurrently with a rise in photocurrent from the electrode. This drop in the EFISH response of the interface is attributed to the decrease in the surface electrostatic fields via the band flattening effect. As the EFISH response is linearly proportional to  $\Delta V_{sc}$ , the drop in SHG intensity can also provide an estimate of the percent band flattening occurring at any applied potential. Similar changes in the surface SHG due to band flattening upon illumination with suprabandgap light have been recently observed from GaAs semiconductor interfaces.<sup>40</sup>

The drop in surface SHG and rise in photocurrent upon UV illumination observed in Figure 4 occurred on a time scale that was faster than the response time of the detection electronics used in the experiments. However, as seen in Figure 4, upon termination of the UV illumination the SHG signal returned

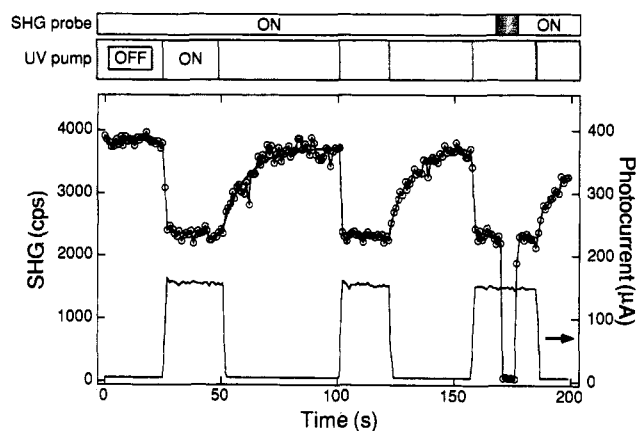


**Figure 4.** SHG (open circles) and photocurrent (solid line) from an n-TiO<sub>2</sub> electrode as a function of time is monitored both with and without illumination from 320-nm (suprabandgap) light while at a potential of +0.5 V vs SSCE. The top bar indicates the on time for the SHG probe beam, while the bottom bar displays the on-off sequence for the UV excitation beam. A long rise time (10–12 s) is observed for the return of the SHG signal after termination of the UV excitation. The supporting electrolyte is 0.3 M NaClO<sub>4</sub> + 10 mM Na<sub>2</sub>HPO<sub>4</sub>, with the buffer set to pH = 7.

slowly (with a time constant of 10–12 s) to its original value. In contrast, the photocurrent from the electrode dropped on a much faster time scale. We attribute this slow return of the EFISH response to the discharging of surface traps for the photogenerated holes; we discuss this effect in more detail in section D.

It is important to note that the drop in surface SHG was only observed if the 584-nm SHG probe beam was overlapped spatially with the 320-nm excitation beam on the electrode surface. This spatial sensitivity confirms that the surface EFISH response is a local probe of the band flattening at the electrode surface. Moreover, band flattening upon illumination cannot be measured during the passage of photocurrent via traditional electrochemical methods. Band flattening has previously been indirectly observed via other optical measurements such as photoluminescence<sup>16,48</sup> and electroreflectance;<sup>21,49</sup> in contrast to those experiments, the SHG directly measures the magnitude of the band flattening by probing the electric fields in the first 20 nm of the space charge region.

The amount of band flattening observed in the surface SHG experiments varied with the power density of the UV (320 nm) beam on the surface. Figure 5 plots the photocurrent and percentage drop in the surface SHG as a function of UV power from 0 to 1.5 mW; in this case the semiconductor electrode is held at a potential of +0.25 V. The photocurrent increased linearly with increasing UV power, whereas the amount of SHG decayed in a logarithmic fashion. The maximum amount of band flattening that could be achieved in these experiments was 70% for the highest power densities of 375 mW cm<sup>-2</sup>. Since these SHG experiments were performed at a fixed potential, the amount of band flattening observed arises from a balance of (i) the rate of electron/hole pair formation and separation with (ii) the rate of hole consumption within the laser spot via either chemical consumption at the electrode surface or electron migration into the laser spot from the rest of the surface. The number of photogenerated charge carriers in the probed surface region can be estimated by relating the measured amount of band flattening to the charge necessary to bring about this voltage change via eq 2. At the highest UV power used, the density of photogenerated carriers in the laser spot was estimated to be on the order of  $3 \times 10^{11}$  e cm<sup>-2</sup>. For the UV power densities employed, the photocurrent is expected to increase linearly with power and the band flattening is expected to have a logarithmic power dependence,<sup>28</sup> in accordance with our measurements.

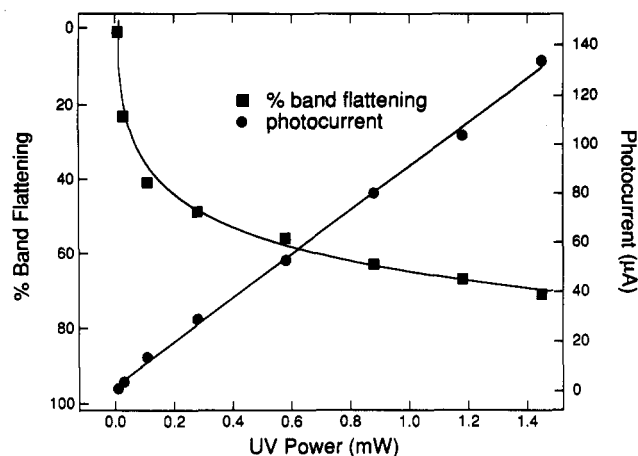


**Figure 5.** Dependence of the photocurrent (circles) and percent band flattening (squares) on the power of the suprabandgap UV excitation beam (320 nm). The maximum UV power corresponds to a power density of 375 mW cm<sup>-2</sup> in a 400-μm spot on the electrode surface. The percent band flattening is the percentage drop in SHG signal upon UV illumination. The photocurrent varies linearly with power, while the band flattening increases in a logarithmic fashion. The electrode was held at a potential of +0.25 V for these experiments, and the supporting electrolyte was 0.3 M NaClO<sub>4</sub> + 10 mM Na<sub>2</sub>HPO<sub>4</sub>.

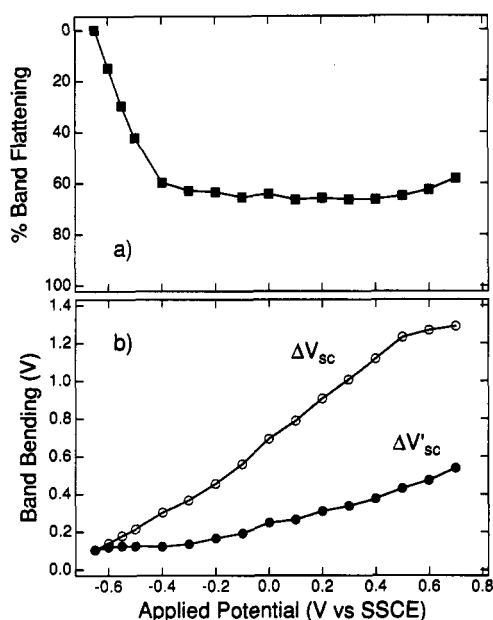


**Figure 6.** (a) Percentage band flattening and (b) the band bending with ( $\Delta V'_{sc}$ , open circles) and without ( $\Delta V_{sc}$ , filled circles) UV illumination. The percent band flattening is obtained from the drop in SHG intensity upon UV illumination at any one potential. The difference in the band bending values with and without illumination is related to the change in the steady-state photogenerated hole concentration at the surface via eq 2.

The amount of band flattening observed in the surface SHG experiments was also a function of the potential of the electrode surface, as shown in Figure 6a. At  $V_{fb}$ , where there were essentially no dc electric fields present at the electrode surface, no drop in the SHG signal and hence no band flattening occurred. As potentials above  $V_{fb}$  were applied, the electrode was driven further into the depletion region and band flattening was observed, reaching a maximum value of 65% at -0.4 V. At potentials above -0.4 V, the percentage drop in the SHG signal and hence the percent band flattening remained constant. Although the percent band flattening remained constant, the absolute amount of band flattening increased with potential.

At any given potential positive of  $V_{fb}$ , the band bending at the electrode surface in the absence of UV illumination can be denoted as  $\Delta V_{sc}$ . As shown in section IIIA,  $\Delta V_{sc}$  can be determined from

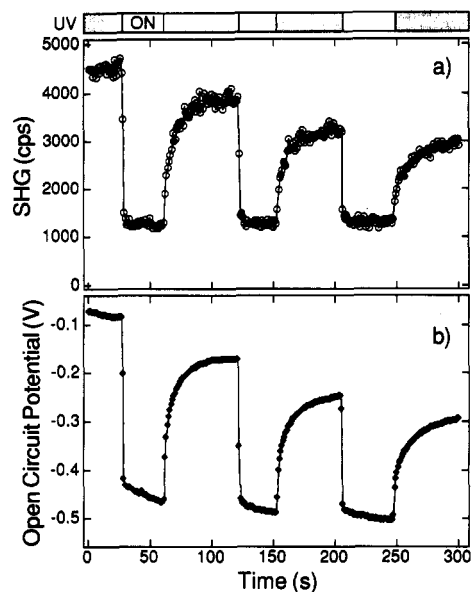


**Figure 7.** (a) SHG signal and (b) rest potential from a n-TiO<sub>2</sub> electrode in an open circuit configuration as a function of time during a sequence of UV illumination periods. As in Figure 3, the top bar indicates the on-off pattern for the UV pump beam. The electrolyte used here was identical to that of Figure 3. The quantitative relationship between the EFISH signal and the rest potential verifies that the SHG experiment is a direct probe of  $\Delta V_{sc}$ .

the SHG intensity measurements. Upon illumination of the electrode with 320-nm light,  $\Delta V_{sc}$  decreases to a new value,  $\Delta V'_{sc}$ , due to the accumulation of photogenerated holes at the electrode surface (band flattening). Figure 6b plots the values of  $\Delta V_{sc}$  and  $\Delta V'_{sc}$  determined from the SHG experiments as a function of the applied electrode potential. Above an applied potential of -0.4 V,  $\Delta V'_{sc}$  increased approximately linearly, but with a different slope than  $\Delta V_{sc}$ . The steady-state photogenerated hole concentration at the electrode surface,  $\Delta q$ , is the difference in charge density at the semiconductor surface due to the UV excitation,  $q_{sc} - q'_{sc}$ . Through eq 2,  $\Delta q$  is proportional to  $(\Delta V_{sc}^{1/2} - \Delta V'_{sc}^{1/2})$  and can therefore be obtained from our optical measurements of the band bending and band flattening at the TiO<sub>2</sub> surface. The steady-state photogenerated hole concentration,  $\Delta q$ , is found to increase from a value of zero at  $V_{fb}$  to a maximum of  $4 \times 10^{11}$  e cm<sup>-2</sup> at +0.5 V.

**C. Band Flattening and Photovoltage Measurements at Open Circuit.** The open circuit photovoltage ( $V_{ocp}$ ) measurement is a standard electrochemical method for characterizing the photoelectrochemical activity of a semiconductor electrode.<sup>2,24</sup> To explore further the relationship between the local decrease in surface SHG from n-TiO<sub>2</sub> electrodes upon UV illumination and the decrease in electrostatic fields at the semiconductor surface, the UV illumination experiments were repeated on the n-TiO<sub>2</sub> electrode at open circuit while simultaneously monitoring the rest potential. Figure 7 plots the SHG and the open circuit potential from the n-TiO<sub>2</sub> electrode as a function of time during three separate illumination periods with UV light. In these experiments, no photocurrents are generated; instead, the rest potential of the electrode changes as charge carriers are generated and accumulate at the electrode surface and as the solution composition is perturbed by the creation of photoproducts. Both the SHG and the rest potential decrease sharply upon illumination, confirming that the changes in the surface SHG are directly related to  $V_{ocp}$ . Because of the linear relationship between the EFISH response and  $\Delta V_{sc}$ , an optically determined photovoltage can be calculated. This calculated voltage agrees precisely with the  $V_{ocp}$  measured electrochemically. The fact that the time dependence of both the SHG signal and the  $V_{ocp}$  are identical also confirms that the same processes are being monitored optically

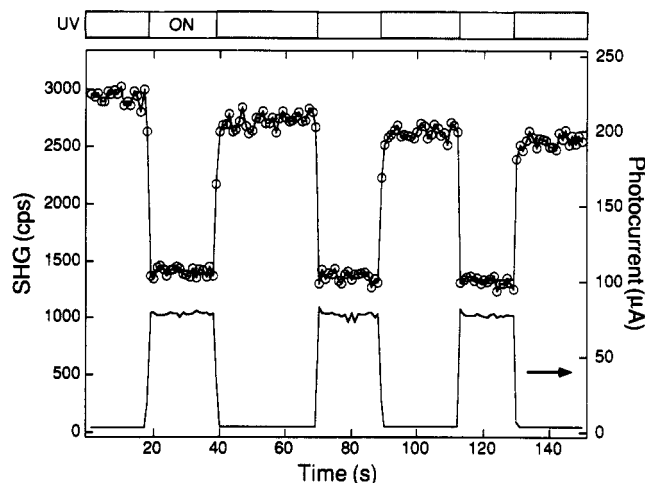


**Figure 8.** Effect of a hole scavenger ( $\text{SO}_3^{2-}$ ) on the SHG rise time after UV illumination. The SHG (open circles) and photocurrent (solid line) are plotted vs time for a n-TiO<sub>2</sub> electrode during a sequence of UV illumination periods, as indicated by the bar above the graph. In this case, the electrode is held at a potential of +0.2 V, and the supporting electrolyte is 0.1 M NaClO<sub>4</sub> + 1 mM Na<sub>2</sub>SO<sub>3</sub> with a pH = 1.5.

and electrochemically. Thus, the open circuit potential measurements conclusively show that the changes in the surface SHG can be quantitatively related to the local changes in the electrostatic fields and band bending at the semiconductor interface. However, it is important to note that the surface SHG obtains a new level upon UV illumination almost instantaneously, whereas the open circuit potential drifts toward a new potential. This is attributed to the fact that the surface SHG is measuring the local voltage within a small (200  $\mu\text{m}$ ) spot on the electrode, whereas the photovoltage is measuring the potential of the entire electrode surface.

When the UV light is blocked, both the surface SHG and the open circuit potential return to higher values with a time constant of 5–10 s. This rise time is similar to that observed in the surface SHG measurements at an applied potential. Note, however, that due to the production of photoproducts in the solution, the rest potential does not return to its original value after the UV beam is blocked. Likewise, the surface SHG does not return to its initial value, once again verifying the relationship between the two measurements.

**D. Surface Trap Discharge Rate.** Having established that the changes in EFISH signal directly correlate with changes in band bending, one of the most interesting discoveries is the long time required for the reestablishment of the equilibrium  $\Delta V_{sc}$  in the laser spot after illumination with UV light, even when an external circuit had fixed the overall potential of the electrode. The SHG returned to its initial value in an exponential fashion with a time constant of  $\approx 10$  s. The rise time for the reestablishment of the electrostatic fields within the illuminated area was very similar for both the open circuit and applied potential measurements. This similarity implies that the surface chemistry and not the external electronics controls the discharge rate of holes at the semiconductor/electrolyte interface.

The effect of surface chemistry on the recovery time of the surface electric fields can be observed by the addition of a hole scavenger sulfite to the electrolyte solution.<sup>50</sup> Figure 8 shows the SHG and photocurrent from the n-TiO<sub>2</sub> electrode in a series of on/off UV illumination experiments similar to those shown in Figure 4, except that the electrolyte solution is now 0.1 M NaClO<sub>4</sub> + 1 mM sodium sulfite at a pH = 1.5. In contrast to the results obtained from the phosphate buffer at a pH = 7, the recovery time of the surface electric fields after illumination is faster than that of the detection electronics (<1 s). A slow loss of SHG from cycle to cycle is also observed and is attributed to the formation of sulfate in the solution, which is found to absorb at the second

harmonic wavelength. This combination of an acidic solution and sodium sulfite resulted in the fastest rise time; low pH values without sulfite resulted in an intermediate rise time, as did sulfite at higher pH values. The long rise times in the presence of phosphate, especially at high pH values, are attributed to the phosphate ion's ability to adsorb onto the oxide surface,<sup>2,13</sup> apparently blocking the reaction of the photogenerated holes on the surface. The decrease in rise time upon addition of the hole scavenger sulfite verifies that the slow chemical discharge of the surface hole concentration after cessation of UV illumination is indeed responsible for the long rise time observed for the return of the surface SHG (and hence  $\Delta V_{sc}$ ) to its equilibrium value.

#### IV. Summary and Conclusions

This paper has described an investigation of the surface electric fields present at a TiO<sub>2</sub> semiconductor electrode during UV excitation using the technique of optical second harmonic generation. When UV light was focused onto the TiO<sub>2</sub> sample, the decrease in electric fields due to the steady-state accumulation of charge at the surface was monitored through the sharp decrease in the EFISH signal. Because of the linear relationship between the EFISH intensity and  $\Delta V_{sc}$ , we were able to report optically determined band flattening values during the passage of current and as a function of applied potential. In an open circuit configuration, it was confirmed that the drop in SHG is a quantitative optical measurement of the electrochemically obtained open circuit photovoltage. After termination of the UV excitation, an unusually long rise time for the return of the EFISH signal to its original value was observed both with an applied potential and in an open circuit configuration. This long rise time was attributed to the presence of surface charge traps and was shown to depend on the surface chemistry at the semiconductor/electrolyte interface.

Due to the direct relationship of the second harmonic intensity to the band bending and the electric fields in the space charge layer, the technique of SHG is capable of straightforward and surface-specific *in situ* measurements of photoelectrochemical processes on n-TiO<sub>2</sub> electrodes. By direct measurements of the surface electric fields, SHG can be used to monitor charge accumulation, charge separation, and charge-transfer events at the TiO<sub>2</sub> semiconductor interface. In a local and time-resolved fashion, the nearly instantaneous response of SHG will be utilized in a subsequent paper to study the establishment of the surface electric fields and charge-transfer processes on a picosecond time scale.<sup>42</sup> In the future, local measurements of the electric field at electrode surfaces can hopefully be used to correlate surface inhomogeneities with areas of distinct surface reactivity. These investigations will aid in the optimization of TiO<sub>2</sub> surfaces as photocatalysts.

**Acknowledgment.** The authors gratefully acknowledge the support of the National Science Foundation in these studies. They also thank Prof. R. J. Hamers for the loan of a HeCd laser used in the comparison experiments and Prof. K. Uosaki of Hokkaido University, Japan, for his generous donation of TiO<sub>2</sub> crystals.

#### References and Notes

- (1) Fujishima, A.; Honda, K. *Nature* **1972**, *238*, 37.
- (2) Finklea, H. O. *Semiconductor Electrodes*; Elsevier: Amsterdam, 1988.
- (3) Nozik, A. J. *Annu. Rev. Phys. Chem.* **1978**, *29*, 189–222.
- (4) Karakitsou, K. E.; Verykios, X. E. *J. Phys. Chem.* **1993**, *97*, 1184–1189.
- (5) *Energy Resources through Photochemistry and Catalysis*; Grätzel, M., Ed.; Academic Press: New York, 1983.
- (6) Heimer, T. A.; Bignozzi, C. A.; Meyer, G. J. *J. Phys. Chem.* **1993**, *97*, 11987–11994.
- (7) Nazeeruddin, M. K.; Kay, A.; Rodicio, I.; Humphry-Baker, R.; Müller, E.; Liska, P.; Vlachopoulos, N.; Grätzel, M. *J. Am. Chem. Soc.* **1993**, *115*, 6382–6390.

- (8) Vinodgopal, K.; Hotchandani, S.; Kamat, P. V. *J. Phys. Chem.* **1993**, *97*, 9040–9044.
- (9) Wang, C.; Heller, A.; Gerisher, H. *J. Am. Chem. Soc.* **1992**, *114*, 5230–5234.
- (10) Mao, K.; Schoneich, C.; Asmus, K. *J. Phys. Chem.* **1992**, *96*, 8522–8529.
- (11) Chazalviel, J. N. *Electrochim. Acta* **1988**, *33*, 461–476.
- (12) Fujishima, A.; Inoue, T.; Honda, K. *J. Am. Chem. Soc.* **1979**, *101*, 5582.
- (13) Noufi, R. N.; Kohl, P. A.; Frank, S. N.; Bard, A. J. *J. Electrochem. Soc.* **1978**, *125*, 246.
- (14) Koval, C.; Howard, J. *Chem. Rev.* **1992**, *92*, 411–433.
- (15) Kasinski, J. J.; Gomez-Jahn, L. A.; Faran, K. J.; Gracewski, S. M.; Miller, R. J. D. *J. Chem. Phys.* **1989**, *90*, 1253–1269.
- (16) Nakato, Y.; Tsumura, A.; Tsobomura, H. *J. Phys. Chem.* **1983**, *87*, 2402–2405.
- (17) Siripala, W.; Tomkiewicz, M. *Phys. Rev. Lett.* **1983**, *50*, 443.
- (18) Fan, F. F.; Bard, A. J. *J. Phys. Chem.* **1990**, *94*, 3761–3766.
- (19) Itaya, K.; Tomita, E. *Chem. Lett.* **1989**, 285–288.
- (20) Uosaki, K.; Kita, H. *J. Electrochem. Soc.* **1983**, *130*, 895.
- (21) Pleskov, Y. V.; Gurevich, Y. Y. *Semiconductor Photoelectrochemistry*; Plenum Publishing: New York, 1986.
- (22) Rhoderick, E. H.; Williams, R. H. *Metal-Semiconductor Contacts*; Clarendon Press: Oxford, 1988.
- (23) Lewis, N. S. *Acc. Chem. Res.* **1990**, *23*, 176–183.
- (24) Lewerenz, H. J. *J. Electroanal. Chem.* **1993**, *356*, 121–143.
- (25) Ponomarev, E. A.; Nogami, G.; Babenko, S. D. *J. Electrochem. Soc.* **1993**, *140*, 2851.
- (26) Salvador, P.; Gutierrez, C. *J. Phys. Chem.* **1984**, *88*, 3696–3698.
- (27) Salvador, P. *J. Phys. Chem.* **1985**, *89*, 3863–3869.
- (28) Kumar, A.; Santangelo, P. G.; Lewis, N. S. *J. Phys. Chem.* **1992**, *96*, 834–842.
- (29) Ferrer, I. J.; Muraki, H.; Salvador, P. *J. Phys. Chem.* **1986**, *90*, 2805.
- (30) Rothenberger, G.; Fitzmaurice, D.; Grätzel, M. *J. Phys. Chem.* **1992**, *96*, 5983–5986.
- (31) Lantz, J. M.; Baba, R.; Corn, R. M. *J. Phys. Chem.* **1993**, *97*, 7392–7395.
- (32) Eisenthal, K. B. *Annu. Rev. Phys. Chem.* **1992**, *43*, 627–661.
- (33) Richmond, G. L. In *Electroanalytical Chemistry*; A. J. Bard, Ed.; Marcel Dekker: New York, 1991; Vol. 17, p 87.
- (34) Corn, R. M.; Higgins, D. A. *Chem. Rev.* **1994**, *94*, 107–125.
- (35) Corn, R. M. *Anal. Chem.* **1991**, *63*, A285.
- (36) Shen, Y. R. *The Principles of Nonlinear Optics*; Wiley: New York, 1984.
- (37) Shen, Y. R. *Annu. Rev. Phys. Chem.* **1989**, *40*, 327–350.
- (38) Heinz, T. F. In *Nonlinear Surface Electromagnetic Phenomena*; Ponath, H. E., Stegeman, G. I., Eds.; North-Holland: Amsterdam, 1991.
- (39) Lee, C. H.; Chang, R. K.; Bloembergen, N. *Phys. Rev. Lett.* **1967**, *18*, 167.
- (40) Qi, J.; Yeganeh, M. S.; Koltover, I.; Yodh, A. G.; Theis, W. M. *Phys. Rev. Lett.* **1993**, *71*, 633–636. In this work, the measured SHG decreases as a function of increasing electric fields in the space charge region. This is due to the fact that the noncentrosymmetric GaAs crystal gives rise to bulk SHG which destructively interferes with the electric field-induced SHG signal. In contrast, the centrosymmetric TiO<sub>2</sub> electrode does not allow for bulk SHG signal in the dipole approximation, and therefore the measured SHG signal is dominated by the electric field-induced SHG, which increases monotonically with increasing electric fields.
- (41) Campbell, D. J.; Higgins, D. A.; Corn, R. M. *J. Phys. Chem.* **1990**, *94*, 3681–3689.
- (42) Lantz, J. M.; Corn, R. M. Manuscript in preparation.
- (43) Guyot-Sionnest, P.; Tadjeddine, A. *J. Chem. Phys.* **1990**, *92*, 734–738.
- (44) Ong, S.; Zhao, X.; Eisenthal, K. B. *Chem. Phys. Lett.* **1992**, *191*, 327–335.
- (45) Corn, R. M.; Romagnoli, M.; Levenson, M. D.; Philpott, M. R. *Chem. Phys. Lett.* **1984**, *106*, 30–35.
- (46) Richmond, G. L. *Chem. Phys. Lett.*, in press.
- (47) Uosaki, K.; Kita, H. In *Modern Aspects of Electrochemistry*; White, R. E., Bockris, J. O., Conway, B. E., Eds.; Plenum Publishing: New York, 1986; Vol. 18.
- (48) Ellis, A. B. In *Chemistry and Structure of Interfaces*; Hall, R. B., Ellis, A. B., Eds.; VCH Publishers: Deerfield Beach, FL, 1986; p 245.
- (49) Hamnett, A.; Lane, R. L.; Trevellick, P. R.; Dennison, S. In *Comprehensive Chemical Kinetics: New Techniques for the Study of Electrodes and Their Reactions*; Compton, R. G., Hamnett, A., Eds.; Elsevier: Oxford, 1989; Vol. 29, pp 385–426.
- (50) Dutoit, E. C.; Cardon, F.; Gomes, W. P. *Ber. Bunsen-Ges. Phys. Chem.* **1976**, *80*, 1285–1288.